THERMOMECHANICAL FINITE ELEMENT ANALYSIS OF HOT WATER BOILER STRUCTURE

by

Dragoljub S. ŽIVKOVIĆ**, Dragan S. MILČIĆ, Milan S. BANIĆ, and Pedja M. MILOSAVLJEVIĆ

Faculty of Mechanical Engineering, University of Niš, Niš, Serbia

Original scientific paper
DOI: 10.2298/TSCI120503177Z

The paper presents an application of the finite elements method for stress and strain analysis of the hot water boiler structure. The aim of the research was to investigate the influence of the boiler scale on the thermal stresses and strains of the structure of hot water boilers. Results show that maximum thermal stresses appear in the zone of the pipe carrying wall of the first reversing chamber. This indicates that the most critical part of the boiler are weld spots of the smoke pipes and pipe carrying plate, which in the case of significant scale deposits can lead to cracks in the welds and water leakage from the boiler. The non-linear effects were taken into account by defining the bilinear isotropic hardening model for all boiler elements. Temperature dependency was defined for all relevant material properties, i. e. isotropic coefficient of thermal expansion, Young's modulus, and isotropic thermal conductivity. The verification of the FEA model was performed by comparing the measured deformations of the hot water boiler with the simulation results. As a reference object, a Viessmann-Vitomax 200 HW boiler was used, with the installed power of 18.2 MW. CAD modeling was done within the Autodesk Inventor, and stress and strain analysis was performed in the ANSYS software.

Key words: *thermomechanical analysis, hot water three-pass fire tube boiler, finite elements analysis*

Introduction

This paper presents a thermo-mechanical analysis of a hot water three-pass fire tube boiler. Such boilers are widespread in the range of large water volume boilers. Combustion of liquid or gas fuel takes place in a Fox corrugated flue, which transfers heat mostly by radiation. The Fox corrugated flue has a wavy shape which reduces strain in the boiler shells caused by various dilatations of the cylindrical layer and the corrugated flue. The reversing chamber on the back of the boiler directs flue gasses to turn for 180^{o} and pass through flue gas tubes of the second wind-box and then through the flue gas tubes of the third wind-box.

Main properties of these boilers are: large radiated area of the corrugated flue, high speed of the combustion products in the flue gas tubes enabling intensive convective heat transfer, compact boiler construction, satisfactory water circulation, and high storage capacity

* Corresponding author; e-mail: dzivkovic@masfak.ni.ac.rs

[1]. Hot water boilers represent highly tensioned thermal-energy facilities. The strain is caused mostly by the operating temperatures which reach the highest values in the area of the corrugated flue, as well as by the hydraulic load.

In the past few years, a couple of accidents have occurred on this type of boilers produced by different manufacturers. The final outcome was water leakage into the gas line of the boiler, causing boiler shutdown. Accidents have occurred on boilers manufactured by both domestic and foreign boiler manufacturers. For the purpose of strengthening the back boiler shells, hot water manufacturers imply various measures such as: increased boiler shell thickness, stiffening boiler shells using horizontal-vertical or radial rims or by stay tubes which connect the back boiler shell with the elements of the reversing chamber [2-4].

Fulfilling the demands of supply and boiler water is of utmost importance with this type of boilers, since this is vital for proper operation and durability of the boiler facility or the district heating system, and has significant influence on the economy of hot water production. Due to scale contamination of heat exchange boiler surfaces, caused by the boiler water of inadequate quality, a drastic reduction of the heat conduction coefficient occurs, with the accumulation of large quantity of energy in the boiler structure. This leads to reduced boiler efficiency and additional thermal strain on the boiler structure.

The aim of this paper was to use thermo-mechanical analysis and finite element method (analysis) – FEM(A) to investigate the state of strains and stresses of a hot water boiler with scale contamination formed by mineral material. Viesmann-Vitomax 200 HV M238, with 18.2 MW of heating power, was chosen as the referent object of investigation. Stress and strain analysis based on FEA was conducted using the ANSYS Workbench 13 software.

Finite elements analysis

The basic idea of FEA is to find a numerical, approximate solution for a complex structural construction [5-10]. The continuum of the construction is idealized and discretized with small, regular 3-D solids that are called finite elements. Finite elements are bonded one to another over mutual nodes and the number of nodes is in direct proportion with the density of finite elements in the continuum and the size of the finite elements. The higher the finite elements density, the smaller the possibility to miss extreme values of stresses in the discretization process is. That is the main principle behind the necessity to increase the density of elements where extreme values of stresses are expected.

The change of influencing parameters within finite elements is described with simple approximation functions. Parameters of the interpolation functions are defined over values of the parameters in the nodes. The strain field of the nodes is estimated as a solution of the matrix equilibrium equation. Based on the strain field, deformation and stress fields are determined, as well as the stress at structure points.

FE analysis procedure for elastic problems

Strain and stresses of hot water boiler structural members are obtained by a static calculation. Thermal calculation is performed based on a given node temperature field. Temperature load is calculated according to the temperature difference in the elements and properties of the material and converted to the equivalent load acting on the nodes.

Basic static equation in the matrix form for a global co-ordinate system [11] is:

$$[\mathrm{K}][u]=[\mathrm{F}] \tag{1}$$

where $[K]$ is the global stiffness matrix, $[u]$ – the global displacement vector, and $[F]$ – the global load vector.

Global stiffness matrix is defined as:

$$[\mathrm{K}]=\sum_{e=1}^{N}[k]_{e} \tag{2}$$

where $[k]_{(e)}$ is the global stiffness matrix of an element, e – the element, and N – the total number of elements.

Global stiffness matrix of an element is defined as:

$$[k]_{(e)}=[\mathrm{T}]^{T}[\hat{\mathrm{k}}]_{(e)}[\mathrm{T}] \tag{3}$$

where [T] is the transformation matrix and $[\hat{\mathrm{k}}]_{(e)}$ – the stiffness matrix of an element for a local co-ordinate system, defined as:

$$[\hat{\mathrm{k}}]_{(e)}=\int_{V}[\mathrm{B}]^{T}[\mathrm{D}][\mathrm{B}]\mathrm{d}V \tag{4}$$

where [D] is the elasticity matrix of the material for the given problem, [B] = [L][N] – the strain-displacement matrix, [L] – the matrix of differential operator, and [N] – the matrix of shape functions.

Global concentrated load of a node may be generated by an outside global concentrated node load $[P_r]$ and local load of all elements $[\hat{f}]_{(e)}$ surrounding the node r transformed into the global load:

$$[\mathrm{F}_r]=[\mathrm{P}_r]+[\mathrm{T}]^{T}[\hat{f}]_{(e)} \tag{5}$$

where

$$[\hat{f}]_{(e)}=\sum_{e=1}^{N}\left(\int_{V}[\mathrm{N}]^{T}[\hat{X}_V]\mathrm{d}V+\int_{S}[\mathrm{N}]^{T}[p]\mathrm{d}S+\int_{V}[\mathrm{B}]^{T}[\mathrm{D}][\varepsilon_T]\mathrm{d}V\right)_{(e)} \tag{6}$$

where $[\hat{X}_V]=q_0$ is the specific element continual load, and $[\varepsilon_T]$ – the thermal strain vector [12].

Terms on the right hand side of eq. (6) represent outside continuous volumetric, surface, and initial temperature loads of an element.

Equations of the static equilibrium represent a system of linear algebraic equations with unknown node displacements. These equations are solved by a direct or iterative procedure. Upon solving the global node displacement, the matrix of transformation defines the vector of element movement $[\hat{u}]_{e}$ in the local coordinate system, as:

$$[\hat{u}]_{e}=[\mathrm{T}][u]_{e} \tag{7}$$

This is followed by determination of the stress vector of the finite element $[\sigma]_{(e)}$ and the strain vector of the finite element $[\varepsilon]_{(e)}$:

$$[\sigma]_e = [\mathrm{D}]\ [\varepsilon]_e - [\varepsilon_T]_e = [\mathrm{D}]\ [\mathrm{B}][\hat{u}]_e - [\varepsilon_T]_e \tag{8}$$

$$[\varepsilon]_e = [\mathrm{B}][\hat{u}]_e \tag{9}$$

FE analysis procedure for elastic-plastic problems

For most elastic-plastic problems, closed-form solutions are not possible and numerical solutions are sought via the FE method. Due to the non-linear relationship between the stress [σ] and the strain [ε], eq. (6) is a non-linear equation of strains, and thus a non-linear equation of nodal displacements [u]. Iterative methods are therefore necessary to solve this equation for a given set of external forces. Moreover, because of the deformation history dependence of an elastic-plastic constitutive relation, an incremental analysis following the actual variation of the external forces must be used to trace the history of the displacements, strains and stresses along with the applied external forces.

The structural eq. (1), which now can be written as:

$$[K(u)][u] = [\mathrm{F}] \tag{10}$$

cannot be immediately solved for the nodal displacement [u] because the information needed to construct the stiffness matrix [$K(u)$] is not known in advance. An iterative process is required to obtain [u] and its associated [$K(u)$] such that the product of [$K(u)$] [u] is in equilibrium with [F] [13].

Two types of numerical algorithms are involved in solving this equation for the displacement increment [Δu] and the stress increment [$\Delta\sigma$]. One is the algorithm used for solving the non-linear simultaneous equations for the displacement increment [Δu] (global/equilibrium iterations). Another is the algorithm used to determine the stress increment [$\Delta\sigma$] corresponding to the strain increment [$\Delta\varepsilon$], which is computed from [Δu], at a given stress state and a given deformation history (local iterations). These two algorithms constitute the non-linear FE procedure for elastic-plastic analysis.

Numerical model

The virtual geometric 3-D model of hot water boiler was defined on the basis of the technical documentation for Viessmann Vitomax 200 HW – 18.2 MW hot water boiler, supplied by the boiler manufacturer [13]. Viessmann Vitomax 200 HW is an oil or gas fired high-pressure hot water boiler for permissible flow temperatures up to 205°C and permissible operating pressures of 6.5 to 25 bar – *i. e.* a standard boiler for district heating and industrial applications. A virtual model of the referent hot water boiler was developed in Autodesk Inventor (CAD software).

As the geometric model was symmetric in respect to the plane normal to the ground surface, which passed through the boiler longitudinal axis, and due to the symmetry of the mechanical and thermal loads, the half of the geometric model was removed to the right of the symmetry plane. The concrete foundation was added to the geometric model in order to perform the analysis with a view realistic structure support conditions. The support of hot water boiler structure by concrete foundation was provided by defining the frictional contact pairs between the carrying cradle and concrete foundation. Cross-linking cradle I-profile, closer to reversing chamber, was anchored to the concrete surface, which corresponded to the actual boundary support conditions.

The geometric model was transformed into the discretized FE model with the application of advanced meshing tools capable of creating adaptive discrete models. The discretized model consisted of 765180 nodes, which formed 141187 finite elements. The discretized model of the hot water boiler is given in fig. 1.

The finite elements mesh was shared between thermal and structural analysis with different types of finite elements used for both analyses. The element types used in thermal analysis were Solid 70, 87 and 90, while static structural analysis was performed with Solid 185, 186 and 187. Contacts between solid bodies were modeled by contact elements CONTA174 and TARGE170 [14].

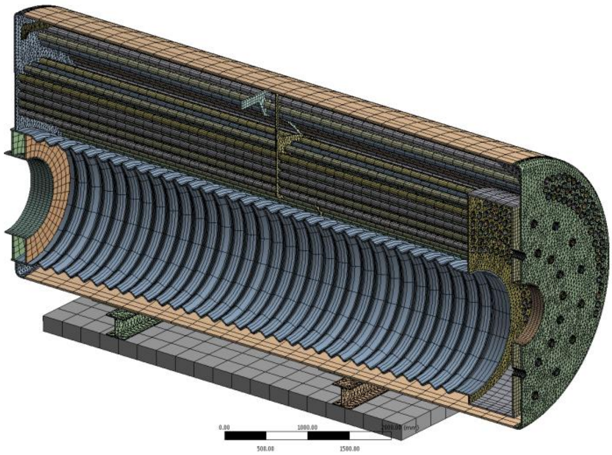

Figure 1. Discretized structure of the hot water boiler

Boundary conditions

The stationary operating regime of Viessmann-Vitomax 200 HW hot water boiler was defined based on the data on nominal operation supplied from the boiler manufacturer [13]. Thermal analysis of the hot water boiler was performed based on the mean temperatures of the heat exchange surfaces on the side of flue gasses and on the side of the water flow – data on the boiler with clean heat exchange surfaces uncontaminated by boiler scale, according to Viessmann (fig. 2) [14].

According to the data supplied by the boiler manufacturer (Viessmann), scale contamination of boiler heat exchange surfaces leads to the increase in mean temperatures of boiler heat exchange surfaces (tab. 1).

Table 1. Wall mean temperatures due to scale contamination [13]

Type of scale contamination	Wall mean temperatures of boiler elements [°C]		
	Corrugated flue Fox	Reversing chamber end front	Smoke tube 2nd pass
1 mm of boiler scale type $CaSO_4$ $\lambda = 2$ [$Wm^{-1}K^{-1}$]	258	239	188
2 mm of boiler scale of type $CaSO_4$ $\lambda = 2$ [$Wm^{-1}K^{-1}$]	404	361	233
1 mm of boiler scale of type Si_xO_y $\lambda = 0,2$ [$Wm^{-1}K^{-1}$]	646	577	322

The results of the previous simulations [16-18] showed that strain-hardening effects due to high deformation and stress concentration of some elements must be included to accurately model a structural boiler analysis. Furthermore, as boiler operates at elevated temperatures, the material model must incorporate temperature effects. The non-linear effects were taken into account by defining the bilinear isotropic hardening effect for all used materials (steels P235GH, P265GH and P295GH). Temperature dependency was defined for all relevant material properties, *i. e*. isotropic coefficient of thermal expansion (fig. 4), Young's modulus (fig. 5), initial yield stress (fig. 3), and isotropic thermal conductivity (fig. 6). Material properties were obtained based on the data supplied by the manufacturers of heat resistant steels [19-21] used in the boiler structure.

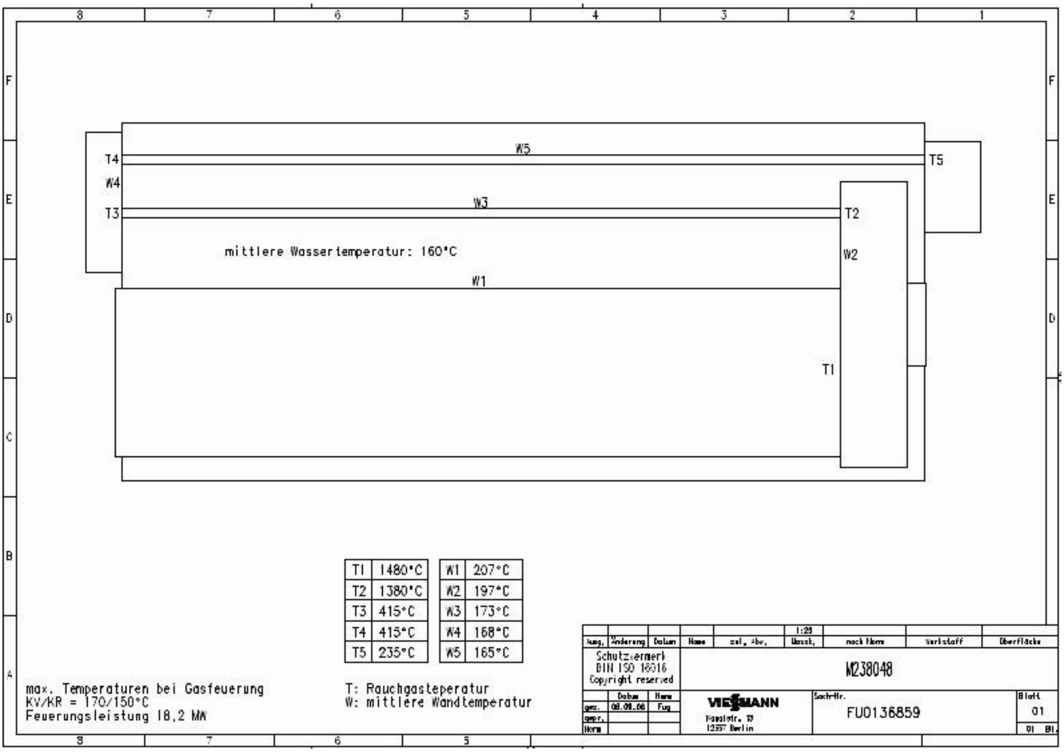

Figure 2. Median temperature used for thermal analysis [13]

Numerical results and discussion

The structural analysis of the hot water boiler was performed in a coupled thermomechanical analysis by the load transfer method. At first, the static thermal analysis was performed in order to obtain the temperature field distribution of hot water boiler structural elements based on the given thermal load. The heat exchange of boiler with a surrounding trough convection and radiation was also taken into account. The resulting temperature distribution was then transferred to the static structural analysis in order to obtain boiler structural component thermal strains.

The FEA simulations were performed for two load cases:

- Case Study 1 – stationary (nominal) load case: hydraulic pressure of 16 bar, thermal load with clean heat exchange surfaces (fig. 2),
- Case Study 2 – operating regime with scale contaminated heat exchange surfaces: hydraulic pressure of 16 bar, thermal load according to tab. 1 (1 mm of boiler scale of type Si_xO_y – λ = 0,2 W/mK.

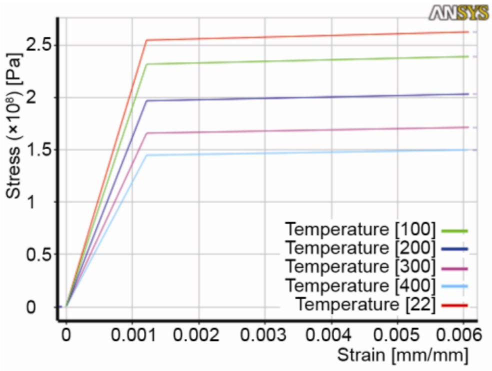

Figure 3. Bilinear isotropic hardening model of steel P265GH

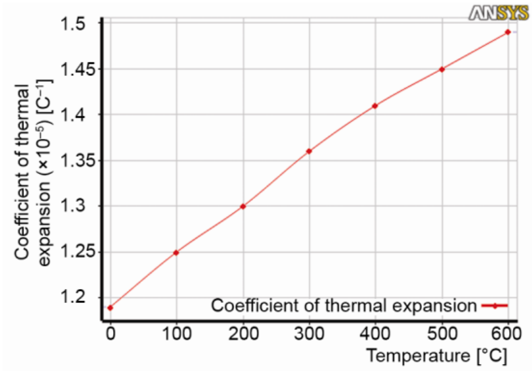

Figure 4. Coefficient of thermal expansion of steel P265GH

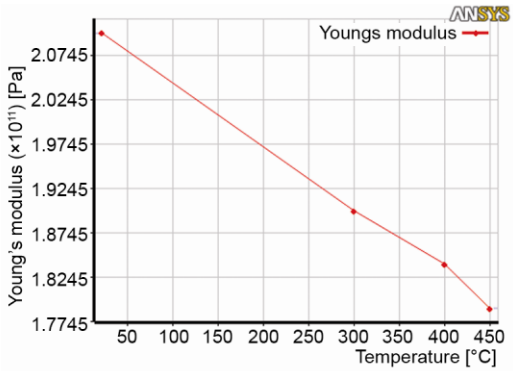

Figure 5. Isotropic elasticity Young's modulus of steel P265GH

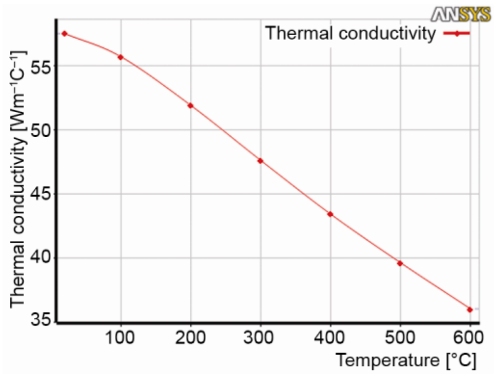

Figure 6. Thermal conductivity coefficient of steel P235GH

Besides thermal and hydraulic pressure loads, other mechanical loads were also taken into consideration during the static structural analysis: the gravity force, the load due to the pressure of flue gas (1 bar), and the hydrostatic water pressure.

Figure 7 shows the total deformation, while fig. 8 shows the equivalent (Von Mises) stresses of the boiler structural elements at nominal operating regime (Case Study 1).

The presented analysis results show that the maximal stresses and deformations occur at the elements of reversing chamber, *i. e*. the reversing chamber end rear and reversing chamber end front, connected by welding with Fox corrugated flue and 2nd pass smoke tubes. The maximal deformation is 9.9935 mm, located at the junction of corrugated flue fox and reversing chamber end front. The maximal equivalent stress is 372.3 MPa, located at the junction of stay tube and the reversing chamber end rear. Maximal stresses in noted place occur due to a sharp edge forming during deformation. As sharp corners in an FEA model cause a stress singularity which cannot be resolved, the noted maximal stresses can be discounted as unrealistically high within a certain distance of the sharp corner. Although the maximal stress values can be discarded, it is obvious that stress concentration at connection between stay tube and the reversing chamber end rear can lead to boiler failure as proved by some authors [3, 17]. Stresses at other boiler structural elements are lower than allowable stresses at elevated temperatures. Perforated reversing chamber end front is one of thermo-mechanically most loaded parts of the boilers with similar design configuration. Figure 9 shows the equivalent stresses, while fig. 10 shows the maximal shear stresses of the reversing chamber end front. The maximal equivalent stress at reversing chamber end front for nominal operating regime is 289.3 MPa.

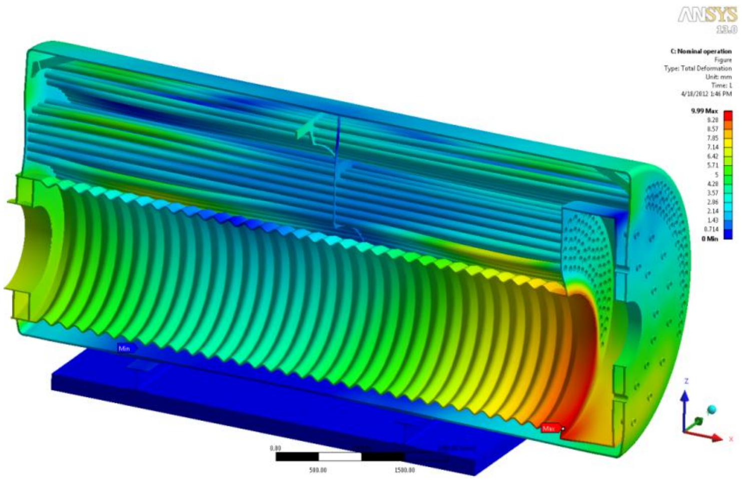

Figure 7. Total deformation of hot water boiler structure at nominal operating regime

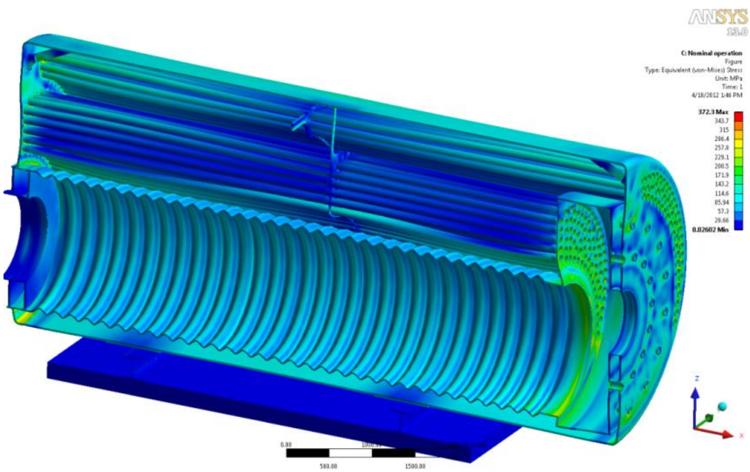

Figure 8. Equivalent stresses of hot water boiler structural elements at nominal operating regime

Maximum stresses in the noted place occur due to a sharp edge forming during deformation, so extreme stress values can be discarded within a certain distance around pipe openings. As Yield strength of the reversing chamber end front is approximately 200 MPa at the temperature of the noted component, it can be concluded that the zone below the second pipe row will certainly plastically deform. Due to strain hardening effects and improvement of material properties at welding zones, the reversing chamber end front and pipe welded connections will hold at nominal operation. But if some of the welded connections in the first two pipe rows (closer to the corrugated flue) are not properly formed, boiler leakage at the noted zone is highly probable.

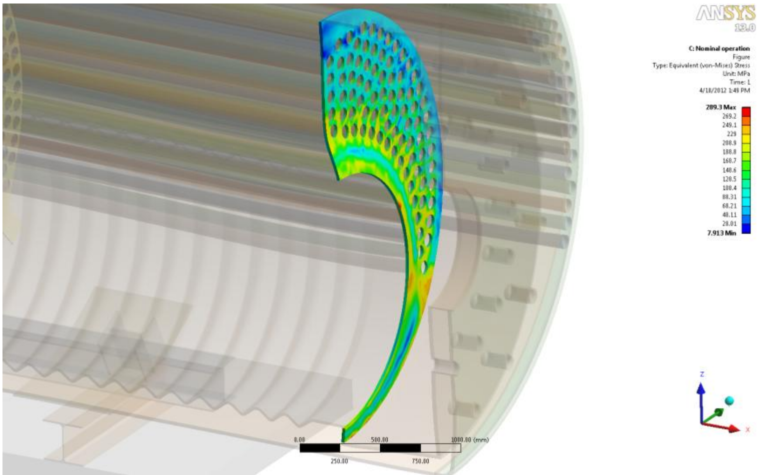

Figure 9. Equivalent stress of the reversing chamber end front at nominal operating regime

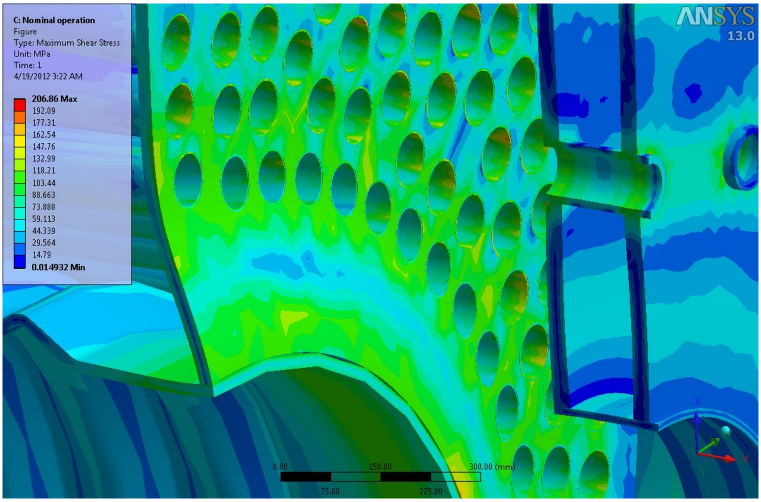

Figure 10. Maximum shear stress of the reversing chamber end front at nominal operating regime

Accidents which have so far occurred in the boilers with similar design, have manifested in the destruction of welded joints between the 2nd pass smoke pipes and reversing chamber end front. The results of the numerical simulations confirm that the most vulnerable part of the boiler is the reversing chamber end front, especially the zone of the first two pipe rows located closer to the corrugated flue fox. Figure 11 shows plastic deformations of Viessmann 200 HW hot water boiler with rated power 18.2 MW after the boiler accident caused by scale contamination of the boiler heat exchange surfaces from the water side. The boiler accident was a consequence of breakage of welded connection between the 2nd pass smoke pipe and reversing chamber end front, thus causing boiler leakage [15].

As already noted, the simulation of hot water boiler behavior with scale contaminated heat exchange surfaces was performed for the worst possible boundary case, *i. e.* the maximal thermal load (Case Study 2). The total deformation and equivalent stresses for Case Study 2 are given in fig. 12 through 14.

The obtained numerical results were indirectly compared with the results obtained by measuring the geometrical parameters of the real boiler (fig. 11, [16]). The actual deformation of reversing chamber end front is very similar to the total deformation obtained through the numerical procedure (fig. 12).

Figure 11. Deformation of the reversing chamber end front

It can be seen from the simulation results shown in figs. 12-14 that scale deposits caused an increase in the total deformation of reversing chamber end front at the critical zone of almost 4 times the value, while equivalent stresses decreased for approximately 90 MPa.

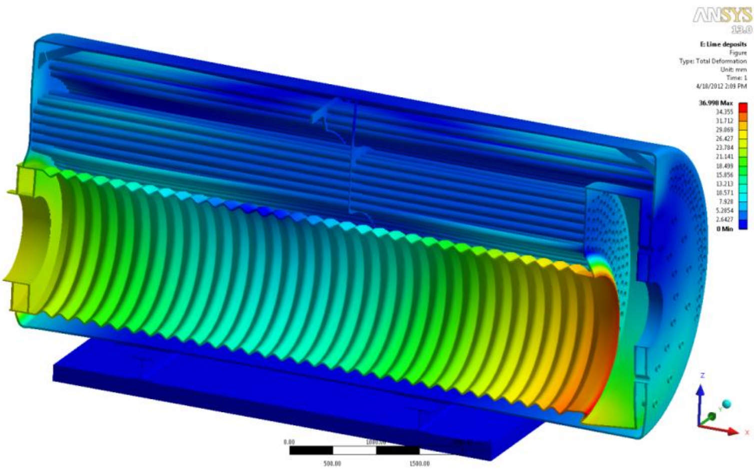

Figure 12. Total deformation of boiler structure with scale contaminated heat exchange surfaces

As Yield strength of reversing chamber end front material (P265GH) at temperatures which correspond to scale contaminated surfaces (577 °C) is approximately 110 MPa, it can be concluded from the analysis of simulation results that equivalent stresses are far beyond the Yield limit (fig. 13). More than 50% of reversing chamber end front is excessively plastically deformed, which may explain the equivalent stress drop in regard to Case Study 1 (nominal operating state). Although the stress concentration due to sharp edge forming under load (and thus singularity of the FE model) can be neglected around the first pipe row, excessive plastic deformation and well above Yield strength will certainly lead to boiler accidents in the noted operating conditions (fig. 14).

The obtained results confirm the current findings that the hot water boilers of this design are highly loaded and that they are particularly sensitive to contamination, *i. e.* creation of a scale layer at boiler heat exchange surfaces. This imposes the requirement that users of such boilers pay particular attention to the quality of the boiler water supply.

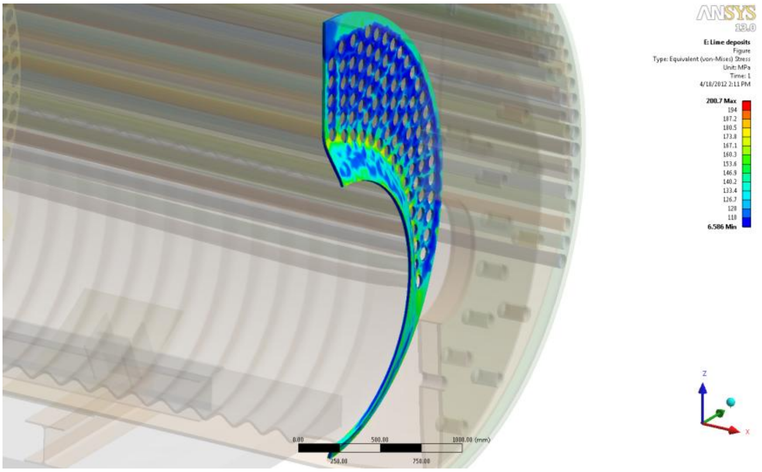

Figure 13. Equivalent stresses of the reversing chamber end front at scale contaminated heat exchange surfaces

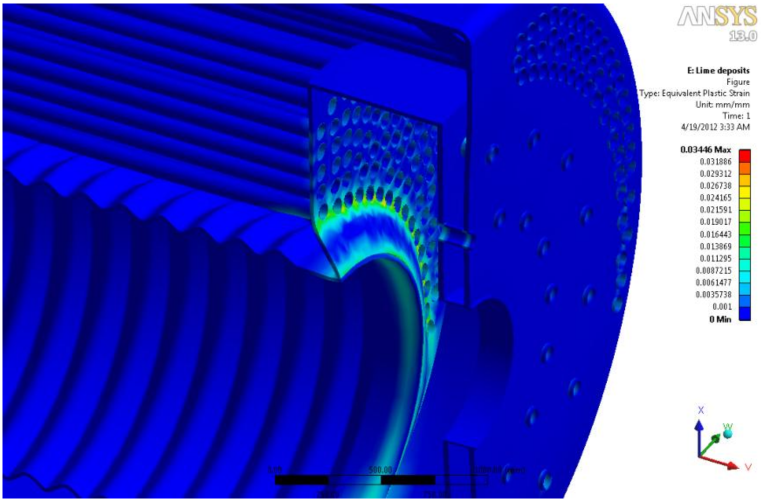

Figure 14. Equivalent plastic strain of the reversing chamber end front at scale contaminated heat exchange surfaces

Conclusions

The main goal of the paper was to investigate the influence of the boiler scale contamination on the thermal stresses and strain in the structure of the hot water boilers.

Simulation results indicate that the part of the boiler under the greatest load is the area of the first reversing chamber, precisely the reversing chamber end rear and reversing chamber end front, connected by welding with corrugated flue and 2nd pass smoke tubes. The welded joints between the smoke pipes and reversing chamber end front are most endangered, as the significant scale deposits can lead to cracks in the welds and water leakage from the boiler.

The obtained results confirm the previous knowledge that hot water boilers of this type are subjected to high strain, and that they are especially sensitive to formation of a scale layer on the heat exchange surfaces, or to dirt in the boiler water.

The methodology presented for thermo-mechanical analysis of the hot water boiler structure may be useful for:
– Manufacturers of hot water boilers, for further design improvements and definition of conditions necessary for their proper operation,
– Users of hot water boilers, for investigating the behavior of the boilers in various operating regimes,
– Insurance companies, for potential risk analysis.

References

[1] Gulič, M., Brkić, Lj., Perunović, P., *Steam boilers,* Faculty of Mechanical Engineering, University of Belgrade, Belgrade, 1991
[2] Gaćeša, B. M., Termo-Mechanical Analysis of Boiler Construction by Numerical Method Applied, M. Sc. thesis, Faculty of Mechanical Engineering, University of Belgrade, Belgrade, 2000
[3] Gaćeša, B., *et al.*, Numerical and Experimental Strength Analysis of Fire-Tube Boiler Construction, *Technical Gazette, 18* (2011), 2, pp. 237-242
[4] Gaćeša, B., Analysis of the Fire Tube Geometry Influence on Boiler Construction Behaviour, *Proceedings,* 37th International Congress on Heating, Refrigerating and Air-Conditioning, SMEITS, Belgrade, 2006, pp. 103-108
[5] Zienkiewich, O. C., Taylor, R. L., *The Finite Element Method,* 5th ed., Butterworth-Heinemann, 2000
[6] Bathe, K. J., *Finite Element Procedures in Engineering Analysis,* Prentice Hall, 1982
[7] Timoshenko, S., Goodier, J., *Theory of Elasticity,* 3rd ed., McGraw-Hill, New York, 1970
[8] Finlayson, B. A., *The Method of Weighted Residuals and Variational Principles,* Academic press, New York, 1972
[9] Nowacki, W., *Thermoelasticity,* Pergamon Press, Oxford, UK, 1986
[10] Kovalenko, A. D., *Thermoelasticity* (in Russian), Science Academy, USSR, Kiev, 1970
[11] Logan, D. L., *A First Course in the Finite Element Method Using Algor,* PWS Publising Company, Boston, 1997
[12] Čukić, R., Naerlović-Veljković, N., Šumarac, D., *Thermoelasticity,* Faculty of Mechanical Engineering, University of Belgrade, Belgrade, 1993
[13] Taqieddin, Z. N., Elasto-Plastic and Damage Modeling of Reinforced Concrete, Ph. D. thesis, Louisiana State University, Baton Rouge, La., USA, 2008
[14] ***, Documentation for Hot Water Boiler Viessmann HW M238 – 18.2 MW, Viessmann, 2010
[15] ***, ANSYS Release 13.0, Documentation for ANSYS, 2011
[16] Milčić, D., *et al.*, Finite Element Thermal Analysis of Hot Water Boilers, *Proceedings,* 14th Symposium on Thermal Science and Engineering of Serbia, Sokobanja, Serbia, 2009
[17] Milčić, D., *et al.*, Stress and Strain Calculation of the Hot Water Boiler's Structure with Application of the FEA, Procesing 2009, 22nd International Congress on Process Industry, Book of Abstracts, Belgrade 2009, pp. 46
[18] Živković, D. S. *et al.*, Numerical Method Application for Thermo-Mechanical Analysis of Hot Water Boilers Construction, *Proceedings,* ECOS 2011 – 24th International Conference on Efficiency, Cost, Optimization, Simulation and Environmental Impact of Energy Systems, Novi Sad, Serbia, 2011, pp. 1351-1362
[19] ***, ThyssenKrupp Materials International, Seamless Carbon Steel Pipe for High-Temperature Service, 2011, www.s-k-h.com
[20] ***, Lucefin Group, Tehnical Card – P235GH, 2011, www.lucefin.com
[21] ***, Salzgitter Flachstahl, Heat-Resistant Pressure-Vessel Steels, 2010, www.salzgitter-flachstahl.de

Paper submitted: May 3, 2012
Paper revised: July 2, 2012
Paper accepted: July 10, 2012